Group: Magnetohydrodynamics

Magnetohydrodynamics for liquid-metal blankets

L. Bühler, H.-J. Brinkmann, C. Courtessole, V. Klüber, C. Köhly, C. Mistrangelo

Liquid metal blanket concepts foreseen in a DEMOnstration nuclear fusion reactor or as test blanket modules (TBM) in the experimental reactor ITER use the lead lithium alloy PbLi as breeder, neutron multiplier, neutron shield and as coolant to remove the volumetrically generated heat. The movement of the electrically conducting fluid in the strong magnetic field induces electric currents responsible for strong Lorentz forces, high magnetohydrodynamic (MHD) pressure drop with implications on heat and mass transfer. The physical parameters characterizing the MHD flow are the Hartmann number and the Reynolds number,

$$Ha = BL\sqrt{\frac{\sigma}{\rho\nu}}, \quad Re = \frac{u_0 L}{\nu},$$

where B, L and u_0 denote magnetic field, typical length scale and velocity. The fluid properties are the density ρ, kinematic viscosity ν and electric conductivity σ. Ha^2 und Re stand for the ratio of electromagnetic to viscous forces and inertia to viscous forces, respectively. For problems, where buoyancy forces are important, the latter ones are quantified by the Grashof number

$$Gr = \frac{g\beta\Delta T L^3}{\nu^2},$$

where ΔT is a typical temperature difference, g stands for gravity and β is the thermal expansion coefficient of the liquid metal.

The MHD work at IKET KIT supports blanket engineering activities of the EUROfusion consortium and the test blanket program of Fusion For Energy (F4E) for ITER.

MHD flows

Optimum grids for MHD simulations

Phenomena imposed by high transverse magnetic fields result in strong electric current density and steep gradients of velocity across extremely thin boundary layers. The later have to be spatially well resolved in numerical simulations since they determine essentially the flow in the entire duct. In contrast, the flow in the core shows only moderate or small gradients so that this part of the flow could be simulated with coarser grids. Computational grids based on cubic cells are favorable for finite-volume calculations of MHD flows in rectangular ducts. As shown in Figure 1, by stretching and compressing the grid independently in both transversal directions, block structured cells adapt perfectly to the duct geometry, while preserving a structural order, that benefits to numerical consistency.

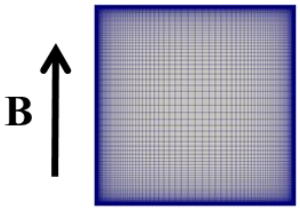

Figure 1: Computational grid for cross section of a rectangular duct MHD flow.

For more complex geometries block-structured grids might not be an optimal choice. Ongoing investigations therefore address the application of unstructured grids for simulations with an in-house-developed MHD code based on the finite-volume library OpenFOAM [1]. One example discussed in the following is the well-known MHD flow in an electrically insulating circular pipe.

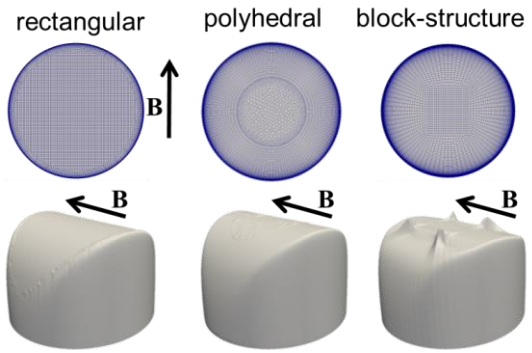

Figure 2: Three grid types for pipe flow and their respective impact on axial MHD velocity profiles (lower row).

Figure 2 shows different types of grids together with their resulting velocity profiles. All grids use hexahedral prisms in order to resolve thin boundary layers, while using rectangular, polyhedral or a block structure in the core. Rectangular and polyhedral based meshes show correct MHD velocity profiles for circular pipe flow. We observe only minor ripples at positions with locally unstructured cells. The block-structured configuration (standard O-grid), however, exhibits large singularities emerging from the corners of the quadratic central core grid. These strong perturbations propagate along grid lines into the fluid. This seems to be an intrinsic problem in finite volume calculations as reported in [1] and [2]. According to [3], locations of slope discontinuity, which are characteristic for the block-structured O-grids, lead to zero order errors, independent of the mesh refinement level. Computations of MHD flows and in particular, the strong coupling of hydrodynamic and electrodynamic phenomena amplifies this effect additionally. Consequently, rectangular or polyhedral grids should be the preferred choice for simulations of MHD flows in complex geometries.

3D MHD flows in fusion blankets

The dual coolant lead lithium (DCLL) blanket is one concept investigated in the frame of EUROfusion [4]. In the proposed design, PbLi serves as breeder and as coolant. Since the liquid metal flows at sufficiently large velocity for efficient heat removal, pressure losses related to the occurrence of electromagnetic forces become significant. Magnetohydro-dynamic effects are coupled with thermal phenomena caused by the occurrence of temperature gradients in the fluid due to the presence of a volumetric neutronic heat load.

In order to reduce MHD pressure drop it has been proposed to use insulating flow channel inserts (FCI) to electrically decouple the PbLi flow from the well-conducting walls. Sandwich-type FCIs are considered as a feasible technical option [4] [5] [6] and their electrical conductivity (of the inner protecting sheet) has been taken into account in numerical simulations.

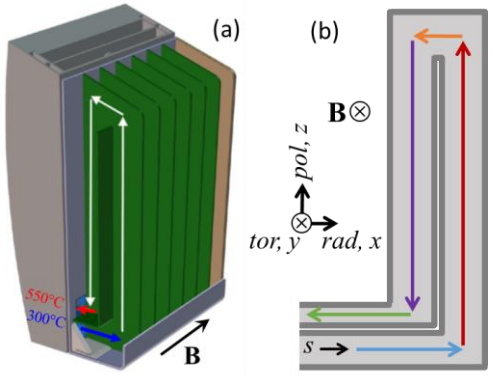

Figure 3: (a) Design of DCLL blanket module. (b) Model geometry for the numerical study.

From Figure 3, it can be noticed that the main characteristic geometric elements of a module area vertical rectangular ducts. Initial numerical simulations for pressure driven flow have been complemented by new 3D calculations for mixed convection of PbLi in the presence of a strong toroidal magnetic field. The flow is driven by an external pressure gradient and by buoyancy associated with the volumetric heating caused by neutrons. A model problem for mixed magneto-convective flow is considered, where a uniform volumetric heat source q in the fluid is assumed. The characteristic temperature difference is related to this heat source as $\Delta T = qL^2/k$, where k stands for the thermal conductivity of the liquid metal. At the entrance, the MHD flow is fully developed and

isothermal. In the inlet duct and in the entire blanket module, the fluid heats up along the flow path as a result of the volumetric heating.

Figure 4 shows results for mixed convection flow at Re= 8596, $Ha = 500$ and $Gr = 10^9$. The temperature distribution on the middle plane at $y = 0$ shows that a high-temperature region is present on the top of the module and in the upper part of the "downward" duct. Streamlines and contours of velocity magnitude depicted in the figure indicate the presence in the rear channel of a descending jet that moves downstream along the internal vertical wall that separates the two poloidal channels. Here the fluid is colder and therefore, due to its higher density, it tends to flow downwards. The downward jet is unstable and this may affect mixing and the heat transfer.

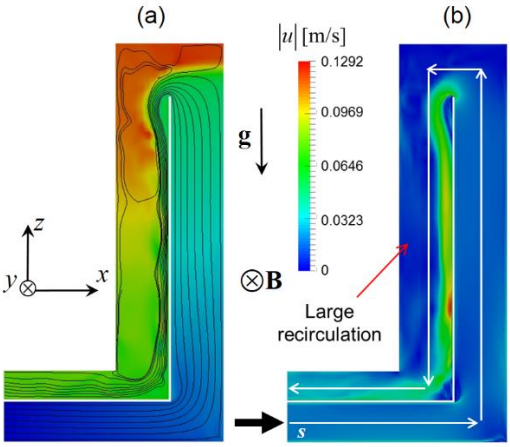

Figure 4: Results for $Re = 8596$ $Ha = 500$ and $Gr = 10^9$ on the plane $y = 0$; (a) contours of temperature and velocity streamlines; (b) contours of velocity magnitude.

Velocity profiles for forced and mixed convection at $Ha = 500$ and $Re = 8596$ are shown in Figure 5 for $Gr = 0$ and $Gr = 10^9$, respectively. The intensity of the downward jet flow at the internal wall can be seen. More details can be found in [7] [8]. Results for magneto convection in geometries related to water cooled lead lithium WCLL blankets are described in [9].

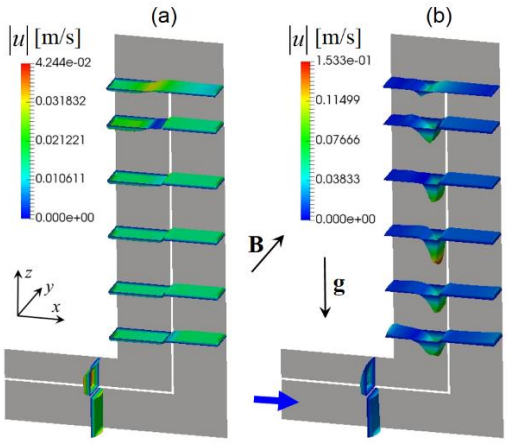

Figure 5: Velocity distributions at different positions along the flow path for MHD flow at $Ha = 500$, $Re = 8596$ for (a) isothermal flow $Gr = 0$, (b) magneto convection at $Gr = 10^9$.

Experimental study of liquid metal MHD flows at the entrance of FCIs

MHD pressure drop in ducts of fusion blankets results from the interaction of flow-induced electric currents with the plasma-confining magnetic field. The highest pressure drop in the flow is observed, when currents shortcut along the thick conducting blanket walls. For reduction of pressure drop, electrically insulating flow channel inserts (FCIs) are foreseen for electrically decoupling the liquid metal flow from the well-conducting channel walls. The preferred option for near-term applications in fusion blankets are sandwich-type FCIs, where the insulating ceramic material is protected from direct contact with the liquid metal by thin sheets of steel. For experimental investigations of 3D effects at the entrance into FCIs and at junctions between two FCIs, a test section has been manufactured and experiments have been performed in the MEKKA facility [10] using NaK as model fluid. The fabrication of FCIs for circular pipes required development of new fabrication strategies [6], since the technology proposed for rectangular ducts [5] did not apply. The experimental study shows the benefits of FCIs for pressure drop reduction in fully developed flows as predicted by theoretical analyses [11] and confirmed by experiments [12].

Details of the experimental test section are shown in Figure 6. The thickness $t_{FCI} = 0.5mm$ of the protection sheets has been suggested e.g. in [13]. The coordinate $x = 0$ corresponds to the position of the pressure tap that is located immediately in front of the FCI. As shown in Figure 6 and Figure 7, the FCI starts at $x = 5mm$ and the insulation inside the FCI at $x_i = 10mm$.

3D perturbations that occur when the flow enters the magnet decay quickly along the flow path as shown in previous investigations [14]. Therefore, the MHD pipe flow is fully developed before the fluid approaches the FCI. In the experiments, pressure and electric potential differences have been recorded and some typical results are discussed in the following.

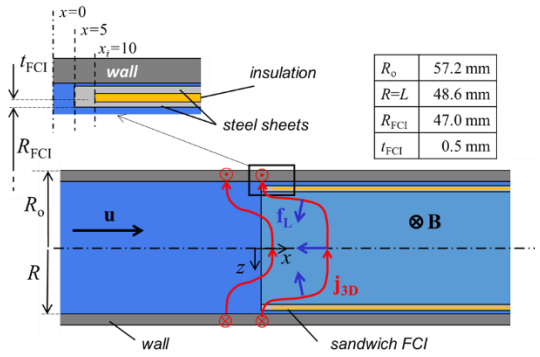

Figure 6: Geometry and principle sketch of current paths at the entrance of a FCI. The insulation inside the FCI starts at $x_i = 10mm$.

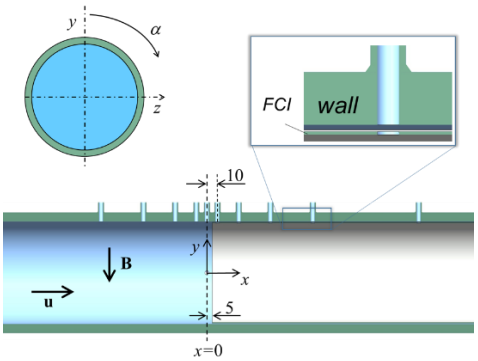

Figure 7: Sketch of FCI position in pipe. The insulating layer inside the FCI (not visible in the sketch) begins at a downstream position of $x_i = 10mm$.

In experiments it is possible to observe a potential difference between both sides of the pipe $\Delta\phi = \phi\left(\alpha = -\frac{\pi}{2}\right) - \phi\left(\alpha = \frac{\pi}{2}\right)$. This quantity is used in the following to investigate the influence of 3D MHD effects at the entrance of the FCI. When potential results are scaled by characteristic values u_0BL, all curves collapse onto a single line as displayed in Figure 8, confirming the universal scaling law for potential over a wide range of Hartmann numbers investigated. Potential values are proportional to the strength of the applied magnetic field and the fluid velocity.

Far upstream, $\Delta\phi(x/L < -2)$ shows fully established conditions with uniform values along x in good agreement with theoretical predictions for fully developed MHD pipe flow [15]. Approaching the FCI, the potential starts monotonically decreasing. At downstream positions, where current paths into the wall are interrupted by the insulation of the FCI, values of $\Delta\phi(x/L)$ decay to zero. We observe that 3D effects, caused by recirculating currents inside the wall near the entrance of the FCI, extend upstream over more than $2L$ and downstream up to $5L$. The currents flowing in the downstream part of the wall are separated from those inside the fluid by the insulation in the FCI. The fact that $\Delta\phi$ vanishes as $x/L > 5$ confirms full functionality of the ceramic insulation inside the sandwich FCI.

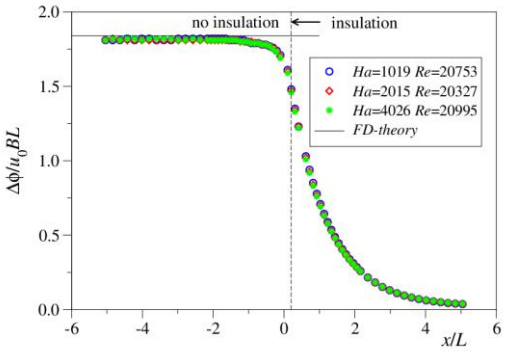

Figure 8: Variation of nondimensional transverse potential difference near the entrance of the FCI.

Pressure differences along the pipe and along the FCI entrance region have been measured for various values of flow rate and for different strengths of the magnetic field. The reference value of pressure has been placed at position $x = x_i$, i.e. $p(x_i) = 0$. When scaled with characteristic quantities $\sigma u_0 B^2 L$, all results come close to a single line as shown in Figure 9. We observe a fast decay of pressure in the bare pipe without insulation and a slower decrease of pressure in the insulated region.

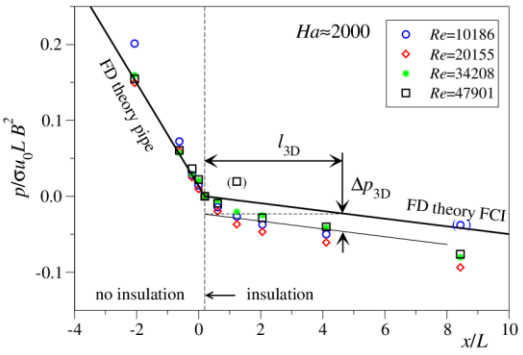

Figure 9: Nondimensional pressure along the axis for $Ha = 2000$ and different.

The pressure gradients in the bare pipe and in the part with FCI agree well with theoretical predictions [16] as indicated by the black solid lines in Figure 9. The FCI reduces the pressure gradient by a factor of about 13.3 compared to the value in the non-insulated pipe. Nevertheless, recirculating additional currents near the entrance of the FCI give rise to extra Lorentz forces that create some additional pressure drop Δp_{3D} caused by 3D effects. Even if the absolute value of Δp_{3D} appears acceptable one should keep in mind that it corresponds to a pressure drop in an ideal long FCI over more than 4 characteristic lengths L. Since similar pressure losses occur also at the exit of the FCI or at gaps between two FCIs [12], these 3D effects reduce the efficiency of FCIs by an amount that is not negligible. For stronger magnetic fields, i.e. higher Hartmann numbers, the behavior is similar. More details can be found in [17].

Design of a MHD mockup experiment of a water cooled lead lithium TBM for ITER

Another concept for an ITER TBM is the water cooled lead lithium (WCLL) blanket [18], where PbLi is employed as breeder and neutron multiplier. Pressurized water cools the first wall and breeding zone (BZ), and EUROFER steel is used as structural material [19]. The design of the WCLL TBM consists of 16 breeder units (BU) arranged in two columns with a complex structure of PbLi and water manifolds (see Figure 10). A system of water cooling pipes placed inside BUs removes the heat generated in the liquid metal. These water pipes are crossing the PbLi manifolds, and they occupy a significant fraction of the manifold cross section. In addition, stiffening plates inside the PbLi manifolds lead to repeated reduction of the cross section and redirect locally the liquid metal flow. The meandering and constricted flow paths increase the PbLi velocity and pressure drop in the manifolds.

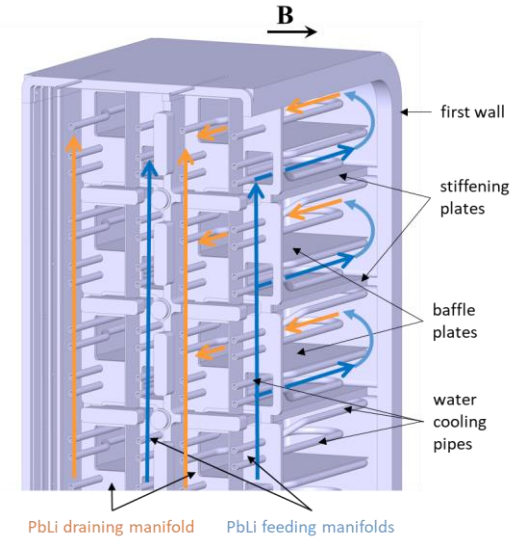

Figure 10: Design of the WCLL TBM as provided by CEA [18]. View on details such as liquid metal manifolds, water pipes, breeder units, baffle plates and stiffening plates.

Objective of the planned experiments is to achieve knowledge about pressure drop in the TBM of the WCLL blanket and to determine the

distribution of the PbLi flow from the manifold into the breeder units. With the aim to investigate the liquid metal flow in a blanket geometry that is most realistic and comparable to the original concept foreseen for ITER, a scaled MHD mockup has been designed on basis of the present WCLL TBM design [18]. In order to achieve high Hartmann numbers in a range relevant for the application, the mockup geometry should be as large as possible. Nevertheless, the mockup has to fit into the gap of the magnet available at the MEKKA facility. To keep the geometry as close as possible to the real design and as large as possible, one column of 8 BUs with distributing and collecting manifolds is considered. With a scale of 1:2.5, such a model geometry fits well into the magnet. It has all geometric features and details, which are necessary for performing meaningful MHD experiments.

For the experiments in the MEKKA laboratory, the WCLL mockup will be embedded with horizontal orientation into the magnet. Figure 11 shows a transparent view of the mockup for visualization of the PbLi flow path showing the main dimensions. The liquid metal is fed into the mock up and removed from it through circular pipes, which are connected to the existing loop in the laboratory. The PbLi is distributed and collected by two manifolds into and out of the BUs. Each BU is fed through a small window in the back wall of the manifolds. The PbLi flow is redirected at the first wall and guided back into the outlet manifold.

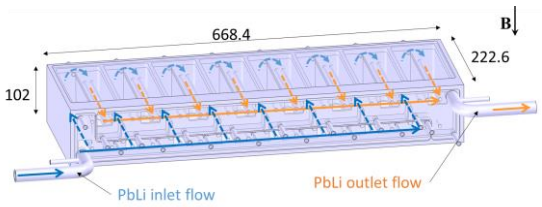

Figure 11: Transparent view of the WCLL MHD mockup design with main dimensions (in mm) and indicated PbLi flow paths.

The WCLL TBM mockup has been simplified to meet manufacturing concerns and to reduce fabrication costs, while keeping the geometry for the liquid metal flow as foreseen in [18]. The test section has been designed with the objective to reduce the number of parts and the number of welds, respectively. An optimized and well-placed number of electron beam welds minimizes welding distortions. Costs for fabrication remain moderate due to the low number of welds.

Details concerning the water flow inside the blanket walls have been omitted since it is expected that they will not affect the liquid metal flow. Water pipes, representing a partial blockage for the liquid metal flow in the manifolds are all present in the mockup.

An exploded view of the mockup in Figure 12 shows the major parts. The main body consists of a single piece, which forms the walls of all BUs, including first wall, stiffening plates, back plate and walls separating the two inlet and outlet manifolds for the PbLi flow. The breeder units are closed from both sides and the manifold is closed by two back plates. The water pipes blocking part of the liquid metal domain are simulated by dummy parts of solid material. All parts are made of 1.4571 austenitic steel that has good compatibility with the used model fluid NaK, and does practically not disturb of the magnetic field.

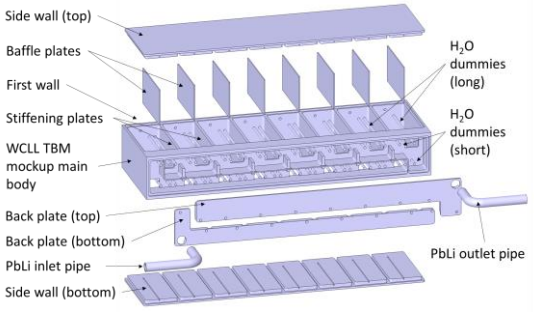

Figure 12: Exploded view of the WCLL MHD mockup with major components: main body, top and bottom walls, back plates as cover for the manifolds, and dummy parts that mimic the water pipes.

Pressure differences will be measured between several points of the mockup using a piping system between pressure taps and the

pressure transducers. The transducers are located outside of the magnet. The piping system is connected with an array of 30 computer-switched valves, which control the measuring sequence. To avoid additional pipes for draining and venting during the filling and emptying process, the positions of the pressure taps have been chosen to also satisfy the function of feeding, draining and venting. They are located at the lowest and highest positions of each breeding unit in the breeding zones and manifolds (see Figure 13).

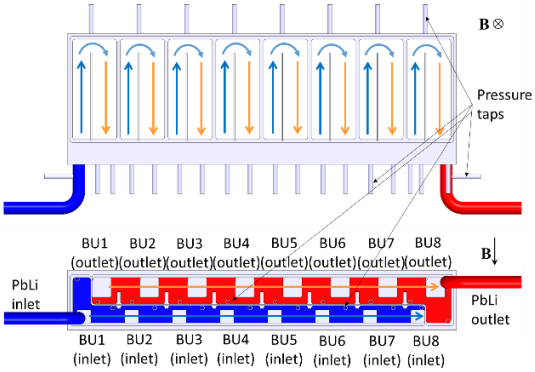

Figure 13: Connections with liquid metal loop and location of pressure taps.

The aim of the planned experiment is to assess MHD pressure losses when the liquid metal passes around obstacles (pipes) and through contractions and expansions. Flows in different parts of the module are electrically coupled since currents induced in one part may leak across electrically conducting walls into neighboring channels. Electromagnetic flow coupling and flow partitioning among BUs is investigated by measurements of the electric potential distribution on the walls.

First experiments in a test section related to magneto-convection in water-cooled lead lithium blankets

The numerous cooling tubes immersed in the liquid metal of a WCLL blanket module create large temperature gradients such that the liquid metal flow, which is partially obstructed by these obstacles, results from the combined interaction of electromagnetic force, buoyancy, and pressure gradient. To improve the understanding of magneto-convective flows, a simplified mockup is used to study buoyant MHD flows in cavities with internal obstacles and to provide a first experimental database for MHD flows with heat transfer in a WCLL-like geometry.

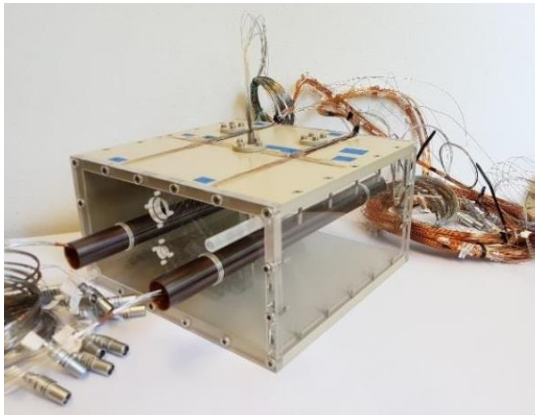

Figure 14: Instrumented test section with transparent walls for preliminary water experiments.

The experimental test section is shown in Figure 14. It was designed to be used with GaInSn as a model fluid and to fit within the gap of the electromagnet present in the MEKKA laboratory. It consists of a rectangular box made of PEEK plastic through which two parallel copper pipes serving as a heat source and a heat sink are inserted. Each pipe is connected to its own temperature-controlled circuit such that they can be kept at constant temperatures T_1 and T_2 during the experiments. This set-up provides the necessary differential heating to establish a horizontal temperature gradient that drives the buoyant flow. The pipes are coated with a 2 µm layer of silicon carbide to electrically insulate the copper from the liquid metal and protect them from corrosion. The test section is fully instrumented to record simultaneously local velocities, electric potential at the walls and temperature at several locations in the fluid. In particular, the temperature distribution in the center of the cavity is measured by

an 11-point thermocouple probe uniformly distributed across the height of the box. Further details are given in [20].

Before proceeding with the liquid metal experimental campaign, preliminary experiments have been performed with water to test the instrumentation and to obtain results for the hydrodynamic limit where no magnet field is applied. Besides, using a transparent medium also enables full flow visualization by optical techniques. For that purpose, two walls of the box were replaced by Plexiglas panels and the water was seeded with fluorescent tracers so that Particle Image Velocimetry can be applied (Figure 15).

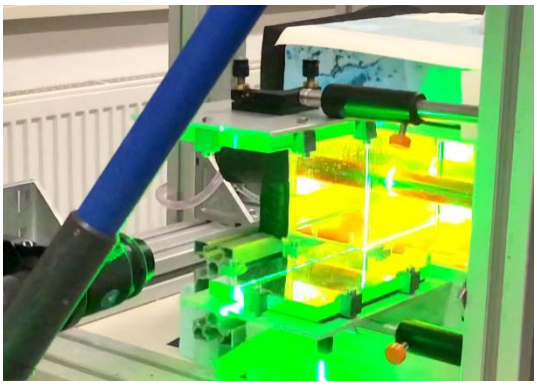

Figure 15: Laser sheet produced by a Nd:YAG laser illuminating the test section during PIV measurements.

Experiments have been performed at various temperature difference $\Delta T = T_2 - T_1$ imposed between the pipes. Results obtained show that the buoyant flow results in a thermal stratification with the hot fluid staying on the top and the cold fluid on the bottom as seen on the dimensionless temperature profiles measured at the central probe and plotted in Figure 16.

$$T^* = \frac{T - \bar{T}}{\Delta T / 2} .$$

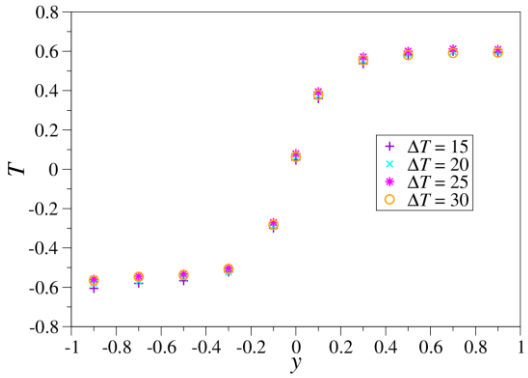

Figure 16: Non-dimensional temperature profile measured at the center of the cavity.

After finishing the preliminary water campaign, the test section will be filled with liquid metal and placed in the magnet to perform experiments for various magnetic fields and temperature differences.

Further work

In addition to the topics described above, the MHD group at IKET KIT contributed in the reporting period 2019 with scientific papers to the development of fusion technology [21] [22] and to fundamental studies of MHD flows [23] [24] [25] [26] [27] [28] [29].

References

[1] Mistrangelo C. and Bühler L.; "Development of a numerical tool to simulate magnetohydrodynamic interactions of liquid metals with strong applied magnetic fields," Fusion Science and Technology, vol. 60, no. 2, pp. 798-803, 2011.

[2] Vantieghem S.; Albets-Chico X. and Knaepen B.; "The velocity profile of laminar MHD flows in circular conducting pipes," Theoretical and Computational Fluid Dynamics, vol. 23, no. 6, pp. 525-533, 2009.

[3] Moukalled, F.; Mangani L. and Darwish M.; The Finite Volume Method in Computational Fluid Dynamics, vol. 113, Springer, 2016.

[4] Rapisarda, D.; Consolidated design of the low temperature EU-DCLL, Presentation at 27th IEEE Symposium On Fusion Engineering (SOFE). 6 June, 2017.

[5] Norajitra, P.; Basuki, W. W.; Gonzalez, M.; Rapisarda, D.; Rohde, M. and Spatafora, L.; "Development of sandwich flow channel inserts for an EU DEMO dual coolant blanket concept," Fusion Science & Technology, vol. 68, no. 3, pp. 501-506, 2015.

[6] Koehly, C. and Bühler, L.; "Fabrication issues of sandwich-like flow channel inserts for circular pipes," Fusion Science and Technology, vol. 72, pp. 660-666, 2017.

[7] Mistrangelo, C.; Büher, L. and Klüber, V.; "Three dimensional magneto convective flows in geometries relevant for DCLL blankets," in 14th International Symposium on Fusion Nuclear Technology, in Budapest, Hungary, September 22- 27, 2019.

[8] Klüber, V. ; Bühler, L. and Mistrangelo, C.; "Numerical simulations of 3D magnetohydrodynamic flows in dual-coolant lead lithium blankets," Fusion Engineering and Design, vol. 146, pp. 684-687, 2019.

[9] Mistrangelo, C.; Bühler, L. and Koehly, C.; "Considerations on magneto-convective flows in model geometries relevant for fusion applications," in Proceedings of the 11th International PAMIR Conference - Fundamental and Applied MHD, July 01 - 05, 2019, Reims, France, 2019.

[10] Barleon, L. ; Mack, K.-J. and Stieglitz, R.; "The MEKKA-facility a flexible tool to investigate MHD-flow phenomena," 1996.

[11] Bühler, L. and Mistrangelo, C.; "Pressure drop and velocity changes in MHD pipe flows due to a local interruption of the insulation," Fusion Engineering and Design, vol. 127, pp. 185-191, 2018.

[12] Bühler, L.; Brinkmann, H.-J. and Koehly, C.; "Experimental study of liquid metal magnetohydrodynamic flows near gaps between flow channel inserts," Fusion Engineering and Design, vol. 146, pp. 1399-1402, 2019.

[13] Urgorri, F.; Smolentsev, S.; Fernandez-Berceruelo, I.; Rapisarda, D.; Palermo, I. and Ibarra, A.; "Magnetohydrodynamic and thermal analysis of PbLi flows in poloidal channels with flow channel insert for the EU-DCLL blanket," Nuclear Fusion, vol. 58, no. 10, p. 106001, 2018.

[14] Bühler, L.; Brinkmann, H.-J. and Mistrangelo, C.; "Experimental investigation of liquid metal pipe flow in a strong non-uniform magnetic field," in Proceedings of the 11th International PAMIR Conference - Fundamental and Applied MHD, July 01 - 05, 2019, Reims, France, 2019.

[15] Miyazaki, K.; Kotake, S.; Yamaoka, N.; Inoue, S. and Fujii-E, Y.; "MHD pressure drop of NaK flow in stainless steel pipe," Nuclear Technology/Fusion, vol. 4, pp. 447-452, 1983.

[16] Miyazaki, V; Konishi, K. and Inoue, S.; "MHD pressure prop of liquid metal flow in circular duct under variable transverse magnetic field," Journal of Nuclear Science and Technology, vol. 28, no. 2, pp. 159-161, 1991.

[17] Bühler, L.; Mistrangelo, C. and Brinkmann, H.-J.; "Experimental investigation of liquid metal MHD flow entering a flow channel insert," Fusion Engineering and Design, vol. 154, p. 111484, 2020.

[18] Batal, T.; Assembly of WCLL TBM: CAD product and parts (by CEA)., personal communication November 27, 2019.

[19] Tassone, A.; Nevo, A. D.; Arena, P.; Bongiovì, G.; Caruso, G.; di Maio, P. A.; di

Gironimo, G.; Eboli, V.; Forgione, N.; Forte, R.; Giannetti, F.; Mariano, G.; Martelli, E.; Moro, F.; Mozzillo, R.; Tarallo, A. and Villari, R.; "Recent Progress in the WCLL Breeding Blanket Design for the DEMO Fusion Reactor," IEEE Transactions on Plasma Science, vol. 46, no. 5, pp. 1446-1457, 2018.

[20] Koehly, C.; Bühler, L. and Mistrangelo, C.; "Design of a test section to analyze magneto-convection effects in WCLL blankets," Fusion Science and Technology, vol. 75, pp. 1010-1015, 2019.

[21] Utili, M.; Bassini, S.; Boccaccini, L.; Bühler, L.; Cismondi, F.; Nevo, A. D;. Eboli, M.; DiFonzo, F.; Hernandez, T.; Wulf, S.; Kordac, M.; Martelli, D.; les Valls, E. M. D;. Melichar, T.; Mistrangelo, C.; Tarantino, M.; Tincani, A. and Vala, L.; "Status of Pb-16Li technologies for European DEMO fusion reactor," Fusion Engineering and Design, vol. 146, pp. 2676-2681, 2019.

[22] Bühler, L.; Mistrangelo, C. and Brinkmann, H.-J.; "Experimental investigation of liquid metal MHD flow entering a flow channel insert," in 14th International Symposium on Fusion Nuclear Technology, in Budapest, Hungary, September 22- 27, 2019.

[23] Klüber, V.; Mistrangelo, C. and Bühler, L.; "Numerical investigation of liquid metal MHD flow in rectangular channels under inclined magnetic fields for fusion relevant parameters," in Proceedings of the 11th International PAMIR Conference - Fundamental and Applied MHD, July 01 - 05, 2019, Reims, France, 2019.

[24] Klüber, V.; Mistrangelo, C. and Bühler, L.; "Numerical investigation of liquid metal MHD flow in rectangular channels under inclined magnetic fields for fusion relevant parameters," Magnetohydrodynamics, p. submitted, 2020.

[25] Klüber, V.; Mistrangelo, C. and Bühler, L.; "Numerical simulation of 3D magnetohydrodynamic liquid metal flow in a spatially varying solenoidal magnetic field," in 14th International Symposium on Fusion Nuclear Technology, in Budapest, Hungary, September 22- 27, 2019.

[26] Klüber, V.; Mistrangelo, C. and Bühler, L.; "Numerical simulation of 3D magneohydrodynamic liquid metal flow in a spatially varying solenoidal magnetic field," Fusion Engineering and Design, p. accepted, 2020.

[27] Bühler, L.; Brinkmann, H.-J. and Mistrangelo, C.; "Experimental investigation of liquid metal pipe flow in a strong non-uniform magnetic field," Magnetohydrodynamics, p. submitted, 2020.

[28] Arlt, T. and Bühler, L.; "Numerical simulation of time-dependent Hunt flows with finite wall conductivity," Magneto-hydrodynamics, vol. 55, no. 3, pp. 319-336, 2019.

[29] Smolentsev, S.; Rhodes, T.; Yan, Y.; Tassone, A.; Mistrangelo, C.; Bühler, L. and Urgorri, C. M. F. R.; "Code-to-code comparison for a PbLi mixed-convection MHD flow," Fusion Science and Technology, p. submitted, 2020.